278

No

MSC INTERNAL NOTE NO. 66-EG-46

PROJECT APOLLO

A STUDY OF LUNAR ORBIT NAVIGATION AND LANDING ACCURACY

Prepared by: Rudolph L. Saldana
Rudolph L. Saldana

Carey F. Lively, Jr.

Robert H. Kidd III
Robert H. Kidd, III

Approved: Kenneth J. Cox
Kenneth J. Cox, Chief
Systems Analysis Branch

Approved: R. G. Chilton
R. G. Chilton, Deputy Chief
Guidance and Control Division

NATIONAL AERONAUTICS AND SPACE ADMINISTRATION

MANNED SPACECRAFT CENTER

HOUSTON, TEXAS

November 16, 1966

INTRODUCTION

The success of the Apollo lunar landing will require a good estimation of the Command Service Module and Lunar Module state vector at the start of powered descent and of the landing site position vector. The purpose of this paper is to compare the accuracy of lunar orbit navigation and landing for the MSFN navigation and the onboard navigation schemes. The accuracy of lunar orbit navigation reflects into the accuracy with which a chosen landing site in a predesignated area can be defined by using two optical sightings. The cost (attitude fuel) and practicality of the onboard navigation system is analyzed. To establish the landing accuracy, an analysis of errors resulting from the Hohmann transfer maneuver, and the powered descent had to be performed. In addition, the uncertainties in the landing site are considered. The estimation of the CSM state for the onboard scheme using recursive linear filter theory is defined in reference 1, and the MSFN capability is obtained from reference 2. The analysis of all LM powered phases is published in reference 3. Reference 4 describes the landing site determination scheme (LSD) examined.

The results of this study are presented in the form of time histories of RMS position and velocity errors during lunar orbit, and standard deviations of position errors, and circular error probability (CEP) at the landing site. RCS attitude fuel, mission timeline, and operational procedures are also presented.

SUMMARY

A study has been made to determine the accuracy of the onboard navigation scheme for the lunar orbit and landing phase of the lunar mission. Further, the onboard orbital navigation accuracy was compared with that available from the manned spaceflight network. The lunar orbit navigational accuracy is reflected into the accuracy of defining a particular landing site in a predesignated area by using two optical sightings (landing site determination scheme). The results of this study indicate (1) that there is little difference between the navigational accuracy associated with the onboard scheme and the MSFN scheme after two orbits, (2) that the landing site determination scheme (LSD) reduces the altitude uncertainties significantly, (3) that a calibration of the LM accelerometers before the Hohmann transfer maneuver is a prerequisite for a $\frac{1}{2}$ nautical mile CEP, and (4) that the onboard navigation techniques appear feasible and requires only a minimal amount of propellant for attitude control.

SCOPE OF STUDY

To determine the capability of the onboard navigation system and compare this capability with that of MSFN, it was necessary to obtain a reference trajectory which contained the essential characteristics of any lunar landing mission. This trajectory started at the lunar orbit insertion and terminated at lunar landing. The nominal sequence of events was taken to be the following:

a. Lunar orbit inertion (LOI) completed at 180° longitude

b. Landmark and/or landing site optical sightings on each orbit

c. 2, 3, or 4 orbits prior to LM descent

d. Hohmann transfer initiation at 167° West longitude requiring 45 seconds

e. Powered descent initiation at 13° East longitude

f. Landing at 0° latitude, 0° longitude

Certain a priori statistics are required for the onboard navigation system to be initialized. The statistics, the error models, and the hardware constraints necessary for the analysis are given in the next section.

ERROR MODELS AND CONSTRAINTS

IMU AND OPTICS

The error model for the IMU and the optical instruments are given in the following figure:

Error Source	Standard Deviation
Gyro Drift	.03°/Hr
Accelerometer Bias	.0066 Ft/Sec^2
With Calibration (Est.)	.0016 Ft/Sec^2
Accelerometer Scale Factor	116 PPM
Scanning Telescope (CSM)	1 MR
Sextant (CSM)	.2 MR
IMU Alinement	.2 MR

Error Source	Standard Deviation
Alinement Optical Telescope (LM)	1 MR
IMU Alinement	1 MR
Optical Tracker (LM)	.2 MR
IMU Alinement	.2 MR

The value for the accelerometer bias after inflight calibration is strictly an estimate and was taken to be one-fourth of the non-calibrated value. The IMU was alined fifteen minutes prior to all powered phases.

MSFN

The MSFN error model and tracking model are given in the following figure:

Station	Noise (Ft/Sec)	Bias (Ft/Sec)	Station Location Uncertainty (Ft) x	y	z
MAD (Master)	.1	.07	128	102	121
CYI	.1	.2	253	453	417
ASC	.1	.2	141	340	358

Assumptions:

(1) Sampling rate at 1/6 Sec for first 10 minutes after acquisition following lunar orbit insertion and 1/minute thereafter.

(2) No a priori information

(3) No data drop out

OPTICS CONSTRAINTS

Constraints on the optical field of view used in landmark tracking are introduced by self-vignetting of the optics and occulsions by the structure.

Shown in figure 1a is the general optical system location and the critical structural limitations in the S/C x-z plane. The structural occulsion is presented in more detail in figure 1b. The self-vignetting limitations are basically a 110° cone for the scanning telescope, and 114° cone for the sextant.

Constraints on the response of the astronaut in performing the landmark sighting function are introduced by the optics control system. The optics line of sight controller is a two channel proportional rate control operated by a controller on the panel. The maximum rate level is adjustable to three levels .1, 1, 10°/sec, which yield a range in rate control available of 50 arc sec/sec to 10°/sec.

LANDMARK UNCERTAINTIES

The landmarks used in the analysis and their associated uncertainties (standard deviations) are given in the following figure:

LANDMARK	Longitude * (degrees)	Mapping Uncertainties (A) (Ft)		Libration Uncertainties (B) (Ft)	Acquisition Uncertainties (C) (Ft)	(A)+(B)+(C) Predicted Uncert. (No orbiter or Surveyor**)		Orbiter Uncertainties	
Messier, B.	48	LAT LON ALT	 2158 2986	1641	3281	LAT LON ALT	 4256 4730	LAT LON ALT	 1748 3609
Toricelli, C.	26	LAT LON ALT	 1554 3281	In Lat, Lon, and Alt For All Landmarks	In Lat, Lon, and Alt For All Landmarks	LAT LON ALT	 3984 4921	FOR ALL LANDMARKS	
Pickering, E.	7	LAT LON ALT	 600 3215			LAT LON ALT	 3718 4878		
Turner	-13	LAT LON ALT	 1067 3281			LAT LON ALT	 3821 4921		
Lansburg, D.	-30	LAT LON ALT	 1554 3281			LAT LON ALT	 3984 4921		

* All landmark latitudes are within $\pm$0.2 degrees of the equator

** Surveyor uncertainties same as predicted uncertainties for all landmarks except E. Pickering (taken to be Surveyor's landing site) which was taken to be 1500 feet in all components

The mapping error (A) results from an inability to accurately map a geographic location on the moon from the earth, and the libration error (B) results from insufficient knowledge of the orientation of the spin axis and spinning rate of the moon. The ability of the astronaut to acquire and mark a point on a land mark (including visual fatigue) is given as the acquisition error (C). The root sum square (RSS) of these three errors were used as the predicted uncertainties. Since an orbiter's mission will be to more accurately map the landmarks from a lunar orbit (decreasing the mapping and acquisition error), the RSS of (A) and (B) of E. Pickering, the minimal mapping error landmark, was used as the orbiter uncertainties for all landmarks. The accuracy with which the surveyor's landing site (taken to be E. Pickering) will be known was used as a landmark uncertainty.

A PRIORI NAVIGATION UNCERTAINTIES

The navigation error covariance matrix at the end of the lunar orbit insertion is the sum of the error resulting from the maneuver itself and the error in the MSFN update prior to the LOI. These covariance matrixes and those for MSFN updates during lunar orbit are given in figure 2.

All data presented both in figure 2 and that which is to follow is given or computed from a locally level coordinate system at the point presented. This is such that z is parallel to the radius vector, x is downrange, and y is to complete the right hand system.

RESULTS AND DISCUSSION

Using the models and data presented in the previous sections, (1) the sighting schedules, (2) the optical instrument used, and (3) the number of orbits before LM separation were varied to determine the effect of each parameter on the accuracy of the lunar orbit navigation and the LM landing. These results are discussed in the following sections.

TWO ORBITS. The onboard navigation capability during two orbits, orbital period 2 hours, is shown in figures 3 and 4. These two plots of RMS position and velocity error illustrate the power of tracking landmarks. Typically, the error grows as the CSM passes the westernmost landmark until arriving at the easternmost landmark. The tracking of this first landmark naturally reduces the error more than any of the remaining landmarks, as can be seen from the figures. This plotted accuracy is the result of sighting three times on each landmark on each pass with the scanning telescope.

This lunar orbit navigation error is reflected into a landing circular error probable (CEP) in figure 5. This landing error is only that resulting from the lunar orbit navigation and hence does not include errors from the LM Hohmann transfer maneuver, the powered descent, nor the landing site itself. The effect of the number of landmarks tracked and the number of sightings on each landmark are shown. The dashed line is the error resulting from an MSFN lunar orbit determination for an update during the second orbit. For

this case of two orbits, it can be seen that the tracking of four or five landmarks is required of the onboard navigation scheme before the resulting landing accuracy is equivalent to that of MSFN.

FOUR ORBITS. The positional lunar orbit navigation capability for four orbits for the onboard scheme and MSFN is shown in figure 6. The onboard scheme assumes a tracking of two landmarks with three measurements each pass with the scanning telescope. This figure indicates that the two navigation accuracies are comparable after two orbits. However, the two peaks in the MSFN error per orbital period indicate that the major MSFN error is an out-of-plane error, while that of the onboard is an in-plane error.

The orbit navigation error is reflected into landing error in figure 7. The additional case of tracking of three landmarks is also given. This resulting accuracy shows the onboard scheme to be slightly better than the MSFN, but this difference should be considered insignificant because both are well within acceptable limits.

THREE ORBITS. The landing accuracy for three orbits is given in figure 8. Additional data are given for sightings with the sextant, which can be considered a variation of the accuracy of the scanning telescope from 1 mr to .2 mr. This figure indicates that MSFN accuracy is between the two landmark and the three landmark for the onboard scheme with the scanning telescope. The discrepancy in the MSFN accuracy for three and four orbits is the result of not having the two MSFN covariance matrices available at the same longitude. This illustrates the problem of determining precise accuracies without a precise timeline for a given mission. As far as landing accuracy is concerned, it is not necessary to have four orbits, for these should be sufficient. Hence, the total landing errors to be presented later will assume three orbits.

LANDING SITE DETERMINATION

Figure 9 shows the geometry of an onboard landing site determination (LSD). The scheme analyzed requires only two sightings on the landing site which are assumed to be taken on the same orbit as LM separation. The solution for the landing site radius vector is given by:

$$\underline{L} = \underline{R} + \left[\frac{(\underline{U}_1 - \underline{U}_2 \cos\phi) \cdot (\underline{R}_2 - \underline{R}_1)}{\sin^2\phi} \right] \underline{U}_1$$

Where:

$\underline{R}_1$ is CSM position at first sighting.

$\underline{R}_2$ is CSM position at second sighting.

$\underline{U}_1$ is the unit vector from $\underline{R}_1$ to $\underline{L}$ obtained from the first sighting.

$\underline{U}_2$ is the unit vector from $\underline{R}_2$ to $\underline{L}$ obtained from the second sighting 1 and $\cos\phi = \underline{U}_1 \cdot \underline{U}_2$.

Figure 10 indicates the errors in the landing site to be expected with and without an onboard LSD. With an onboard LSD, the error in the altitude of the landing site is considerably improved. This is an important achievement because of the ramification of altitude errors on the powered descent guidance. The range error in the landing site with the onboard navigation is high, but could be reduced by the tracking of more landmarks.

HOHMANN TRANSFER AND POWERED DESCENT

Figure 11 shows the landing errors resulting from the Hohmann transfer maneuver and the powered descent. The Hohmann transfer maneuver was assumed to take 45 seconds, which allows for an ullage, a low thrust period, a short high thrust period, and a monitoring of engine cut-off with the inertial measuring unit. The product of this total time with the accelerometer bias is the major error resulting from this maneuver. Since the partial derivative of landing error with respect to horizontal velocity error at the Hohmann transfer point is approximately two miles, this accelerometer bias is a very important error. The three cases considered show the extremes in expected accuracy and indicates that an inflight calibration of the accelerometer bias is prerequisite for meeting a 3,000 feet CEP at landing.

TOTAL LANDING ACCURACY

Figures 12 and 13 indicate the total landing accuracy, which is the sum of the navigation accuracy and the accuracy of the landing site itself. The navigation errors at landing for MSFN or onboard orbit navigation are essentially the same; however, the LSD for the two result in a larger total error for the onboard scheme. For either orbit navigation scheme, there is a significant improvement in the total altitude error which would have to be removed by the guidance system (with the landing radar) during powered descent. It is this improvement which illustrates the importance of the onboard landing site determination.

LUNAR LANDMARK SIGHTING FEASIBILITY

The demonstration of lunar landmark sighting feasibility is dependent on the limitations imposed by spacecraft (S/C) constraints, such as RCS propellant capacity and the capability of the astronaut to recognize, track, and mark the landmark using the optics controller and spacecraft attitude control. Many methods using various combinations of optics control and spacecraft control might be invisioned; however, the reasonable techniques would appear to be those in which the spacecraft attitude is oriented prior to the sighting and the optics line-of-sight is controlled to mark the landmark position.

This study considered several attitude maneuver techniques and comparisons of the attitude techniques on the basis of RCS propellant, earth communication loss, and time in which the landmark (LMK.) was visible to the astronaut in the field of view of the optics. A preferred technique was chosen based on minimizing RCS propellant and communication loss and providing acceptable time for the astronaut to perform the sighting function.

The attitude techniques which were considered are given below.

1. Roll-Yaw Local Vertical (LV) Rate. The spacecraft is oriented with the shaft axis of the optics along the local vertical radius vector with the y body axis in the plane of the orbit. The S/C is given a roll yaw rate equal to the orbital rate. The axis system referred to is the CSM body axis system as shown in figure 1a.

2. Roll LV Rate. The S/C z body axis is oriented along the local vertical radius vector with the S/C y axis in the plane of the orbit and the S/C is given a roll rate equal to orbital rate.

3. Pitch LV Rate. This technique is the same as roll LV except S/C x axis is in the orbit plane.

4. Roll Inertial. The S/C attitude is held inertially fixed as the landmark is tracked, and the S/C is oriented prior to the sighting such that the S/C z body axis is parallel to the radius vector of the landmark to be tracked. The S/C y-z plane is in the orbit plane.

5. Pitch Inertial. This technique is the same as roll inertial, except the S/C x-z plane is in the orbit plane.

6. Roll LMK Rate. The S/C is oriented with the S/C y-z plane in the orbit plane and rotated at a rate to hold the landmark stationary in the optics.

7. Pitch LMK Rate. This technique is the same as roll LMK rate except the S/C x-z plane is in the orbit plane.

A comparison of the LMK attitude techniques is given in figure 14. Landmark observation time, RCS propellant, and loss of earth communication is tabulated. The LMK observation time was derived by considering the S/C in an 80 n.m. circular orbit with an orbital rate of .05°/second; therefore, the time required to traverse a central angle (θ) may be determined. The optics look angle ψ at which a LM appears in view and disappears, was related to θ to determine the LMK observation time. It was assumed that the landmarks will be chosen approximately in the orbital plane; therefore, the optics look angle (ψ angle between the optics line-of-sight and the shaft axis) and look angle rate were related to the central angle (θ - angle between the landmark radius vector and the radius vector to the S/C) through plane geometry. The relationship between ψ and θ are given for the S/C local vertical modes and S/C Inertial Modes in figures 15 and 16 respectively.

Previous Gemini simulation experience has shown approximately 30 seconds required per landmark sighting with 1 minute required for acquisition of the landmark. Since the Apollo optics control is available whereas Gemini did not have this capability the previous numbers are assumed conservative for Apollo. All times listed in figure 14 allow at least four sightings per landmark.

It may be seen from figure 14 that the roll-yaw local vertical rate technique is superior with respect to RCS propellant and communication loss and LM observation time. It has therefore been chosen to illustrate the detail attitude profile required and a detailed breakdown of the RCS propellant requirements. It is the recommended technique on the basis of these considerations; however, it may be seen in figure 14 that the roll LV technique would be acceptable and it would be simpler to implement.

The RCS propellant required for the roll-yaw local vertical mode is shown in figure 17. The RCS propellant was derived from the propellant utilization given in reference 5. The results indicate that 4.84 lbs. of RCS propellant per orbit are required to include landmark sightings using a roll-yaw LV rate technique in the lunar mission. The RCS propellant for landmark sighting on two orbits are compared to previously used landmark sighting techniques and their contribution to the corresponding RCS propellant budgets is given in figure 18.

It may be seen from figure 18 that the cost of landmark sightings on two orbits with this technique is reasonable when compared to the advantages of including landmark sighting to improve the on-board navigational capability.

RECOMMENDED TECHNIQUE AND ATTITUDE TIMELINE

The technique for performing lunar landmark sightings is as follows with the attitude timeline and sequence as shown in figure 19.

1. Orient the S/C and perform the IMU alinement such that this operation is complete at $+90^{\circ}$ lunar longitude.

2. Initiate local vertical rate in roll-yaw or roll at $+90^{\circ}$ longitude.

3. Orient the optics toward the chosen landmark when the S/C is 6° longitude from the landmark.

4. Control the optics line-of-sight at a rate equal to the landmark motion in the optics as shown in figure 15.

5. Repeat 3 and 4 for additional landmarks.

6. Stop local vertical rate after landmark sightings and landing site determination measurements are completed. This occurred at approximately zero degrees longitude for the preliminary mission profile (considered in this study).

7. Orient the spacecraft to reacquire communication.

8. GN&C system may be turned off after Item 7 is completed.

CONCLUSIONS AND RECOMMENDATIONS

The landing sight determination technique will significantly reduce the altitude uncertainty of the lunar landing site and should be incorporated as part of the onboard navigation capability.

The onboard navigation landmark sighting technique is comparable in accuracy with MSFN if two landmarks per orbit with three sightings per landmark are performed on two orbits, and it requires a minimal amount of RCS propellant. These lunar landmark sightings should be incorporated in the lunar mission to provide an alternate lunar navigation capability. A roll-yaw or roll local vertical attitude technique as presented herein should be used for these sightings.

Recalibration of the landmark accelerometer prior to LM/CSM separation is essential with any navigation technique to meet a half mile CEP. This calibration should be performed automatically and should be checked out on early earth orbit missions.

A manual simulation of the lunar landmark sighting phase should be conducted to study the landmark acquisition problem and further define manual procedures.

APPENDIX A

Presented in this section are the equations which were used to determine the landmark sighting time available. The data presented in the text of this report is based on the planar problem where the landmark is in the orbital plane; however, the three dimensional case is also presented herein.

The optics look angles ψ and η were related to the central angle (θ), between the landmark radius vector and the S/C position vector and the out-of-plane angle of the landmark (ϕ). The time available for viewing a landmark may be determined by relating the angle where structural occlusions occur (see figure 1b) to θ at that point. The time necessary to traverse an angle θ is given by the angle between where the landmark appeared and disappeared in the field of view and the orbital rate $\dot{\theta} = -.05^{\circ}/\text{sec}$. which is consistent with an 80 n.m. circular lunar orbit. The time may be determined for any constant out-of-plane angle ϕ. The geometric relationship between optics look angles and location of the landmark, with respect to the spacecraft, is given in figure A.1. The orbital plane contains the L and R axis and the L and P axis contain the landmark (LM). The angles ψ and η correspond to the optical look angles with respect to the S/C radius vector (r) and if the optical axis is coincident with r and the S/C X axis is in the orbital plane, ψ and η correspond to the optical shaft and trunion angles, respectively.

The equations which define ψ, η with respect to ϕ, θ, were obtained from spherical trigonometry, and are as follows

(1) $$\tan\psi = \frac{\sin\beta}{1 + h/r_m - \cos\beta}$$

(2) $$\sin\eta = \frac{\sin\phi}{\sin\beta}$$

(3) $$\cos\beta = \cos\phi\cos\theta$$

(4) $$\sin\beta = +\sqrt{1 - \cos^2\phi\cos^2\theta}$$

where: The angles are defined in figure A.1.

These relationships are presented graphically in figure A.2. The time available for any given out of plane angle ϕ may be obtained from this figure and the optics occlusion constraint given in figure 1.b.

It was assumed in this paper that the landmarks would be chosen very close to the plane of the orbit to maximinize the sighting time and therefore planar relationships were used, i.e., ($\phi = 0$). That this technique yields the maximum observation time may be seen in figure A.2. Two apparent cases are possible: (1) The S/C is rotated at orbital rate to maintain the optics shaft along the S/C radius vector, (2) the S/C shaft axis is oriented parallel to the radius vector of the landmark and maintained stationary. The equation for case (1) is:

$$\tan\psi = \frac{\sin\theta}{1 + \frac{1}{r_m} - \cos\theta} \tag{5}$$

The rate at which the landmark appears to move in the optics is related to orbital rate as follows:

$$\dot{\psi} = \left(\frac{r/r_m \cos\theta - 1}{r/r_m{}^2 - 2\frac{r}{r_m}\cos\theta + 1} \right) \dot{\theta} \tag{6}$$

Case (2). The case where the S/C attitude is inertial is obtained from the relations for Case (1) by

$$\psi_I = \psi + \theta \tag{7}$$

$$\dot{\psi}_I = \dot{\psi} + \dot{\theta} \tag{8}$$

where: ψ_I is the look angle if the optics shaft axis is parallel to the landmark radius vector.

REFERENCES

1. MSC Internal Note No. 66-EG-3, "Apollo Navigational Accuracy in Lunar Orbit Including Landmark Updating."

2. Memorandum 66-FM42-94, "MSFN Navigational Capabilities During the CSM Lunar Parking Orbit."

3. MSC Internal Note No. 65-EG-12, "Position and Velocity Error Covariance Matrices at Thrust Termination for the Apollo LEM."

4. MSC Internal Note No. 66-EG-18, "Determination of LM Landing Site Inertial Type Sighting Coordinates by CSM Landmark."

5. Memorandum (MSC) EG23-23-66, "Propellant Utilization Per Maneuver and Associated Confidence Levels for the CSM/CDR Propellant Requirements Review,"

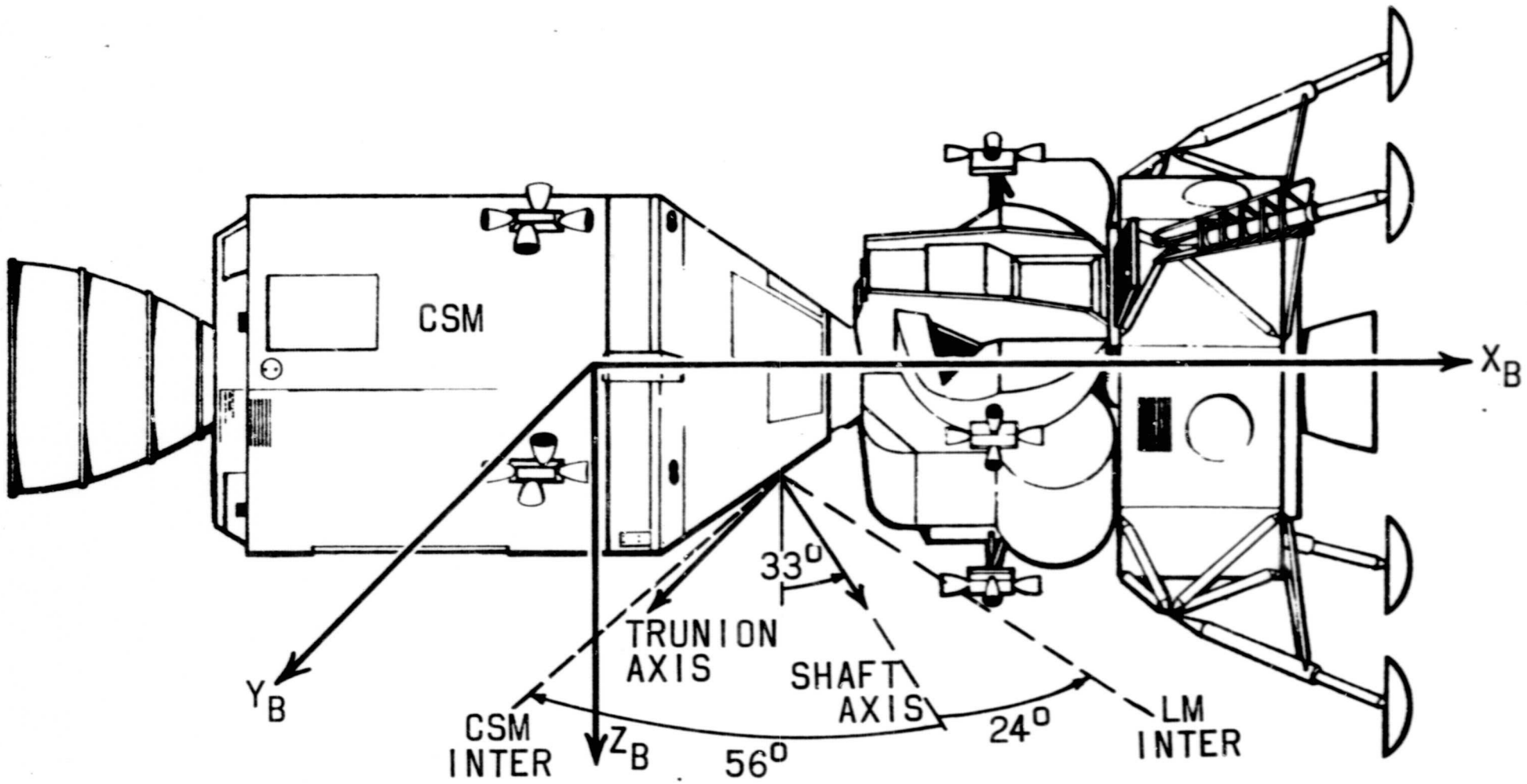

COMMAND MODULE OPTICAL INTERFERENCE

FIGURE 1a

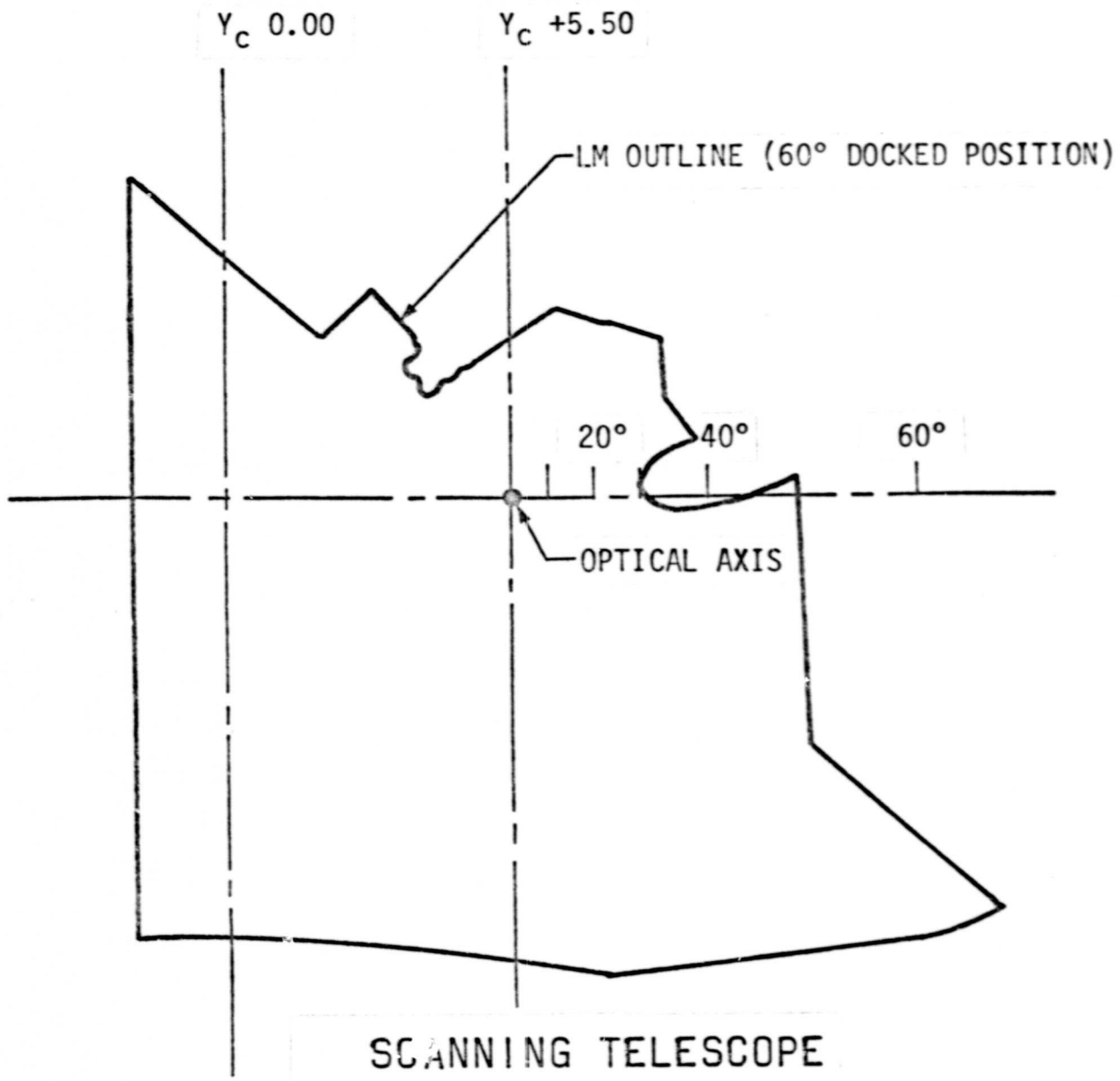

COMMAND MODULE OPTICAL INTERFERENCE

FIGURE 1b

MSFN UPDATE COVARIANCES
FIGURE 2

- MSFN UPDATE COVARIANCE FOR LOI (PROPAGATED TO END OF LOI)

STANDARD DEVIATIONS	X	Y	Z	$\dot{X}$	$\dot{Y}$	$\dot{Z}$
1202.0 ft	1.4457^6	2.568^6	-7.1423^5	460.9	-6452.0	-958.0
3657 ft		1.3374^7	-1.9506^6	1250.0	-33452.0	-1824.0
667.0 ft			4.452^5	-279.2	4881.0	491.6
.434 ft/sec				.1885	-3.131	-.3146
9.12 ft/sec	SYMMETRIC				83.69	4.579
.799 ft/sec						.6388

- LOI MANEUVER ERRORS

STANDARD DEVIATIONS	X	Y	Z	$\dot{X}$	$\dot{Y}$	$\dot{Z}$
390.0 ft	1.5245^5	0.0	6719.0	861.0	0.0	43.186
487.0 ft		2.3779^5	0.0	0.0	1362.0	0.0
540.0 ft			2.699^5	30.79	0.0	1582.0
2.20 ft/sec				4.861	0.0	.2011
2.79 ft/sec	SYMMETRIC				7.806	0.0
3.04 ft/sec						9.279

FIGURE 2 (CONT'D)

- MSFN UPDATE COVARIANCE MATRICES AT SEPARATION

- TWO ORBITS

STANDARD DEVIATIONS		X	Y	Z	$\dot{X}$	$\dot{Y}$	$\dot{Z}$
277.9	ft	7.727^{4}	-1.345^{5}	-1.061^{4}	-9.389	807.7	-88.42
920.1	ft		8.464^{5}	-4.942^{4}	3.908	-2316.0	135.2
989.3	ft			9.787^{3}	3.368	-32.54	15.91
.04487	ft/sec				2.013^{-3}	-.0993	.0125
3.229	ft/sec	SYMMETRIC				10.43	-.9443
.3245	ft/sec						.10536

- THREE ORBITS

STANDARD DEVIATIONS		X	Y	Z	$\dot{X}$	$\dot{Y}$	$\dot{Z}$
244.4	ft	5.9739^{4}	-1.6811^{5}	-2.0589^{4}	.6537	596.9	-82.51
1218.0	ft		1.4834^{6}	-1.0713^{5}	40.93	-2867.0	129.1
186.0	ft			3.4727^{4}	-7.256	-17.39	46.21
4.267^{-2}	ft/sec				1.821^{-3}	-.0434	-5.327^{-3}
2.723	ft/sec	SYMMETRIC				7.412	-.7113
.3546	ft/sec						.12577

- FOUR ORBITS

STANDARD DEVIATIONS		X	Y	Z	$\dot{X}$	$\dot{Y}$	$\dot{Z}$
300.5	ft	9.033^{4}	-659.7	-7.322^{4}	27.95	315.5	-132.1
1069.0	ft		1.144^{6}	-1.011^{5}	56.28	-1630.2	1.424
264.9	ft			7.015^{4}	-28.21	-119.3	109.1
.1077	ft/sec				.01159	.01969	-.04145
1.859	ft/sec					3.457	-.4711
.4420	ft/sec						.19539

ONBOARD LUNAR ORBIT NAVIGATION CAPABILITY

FIGURE 3

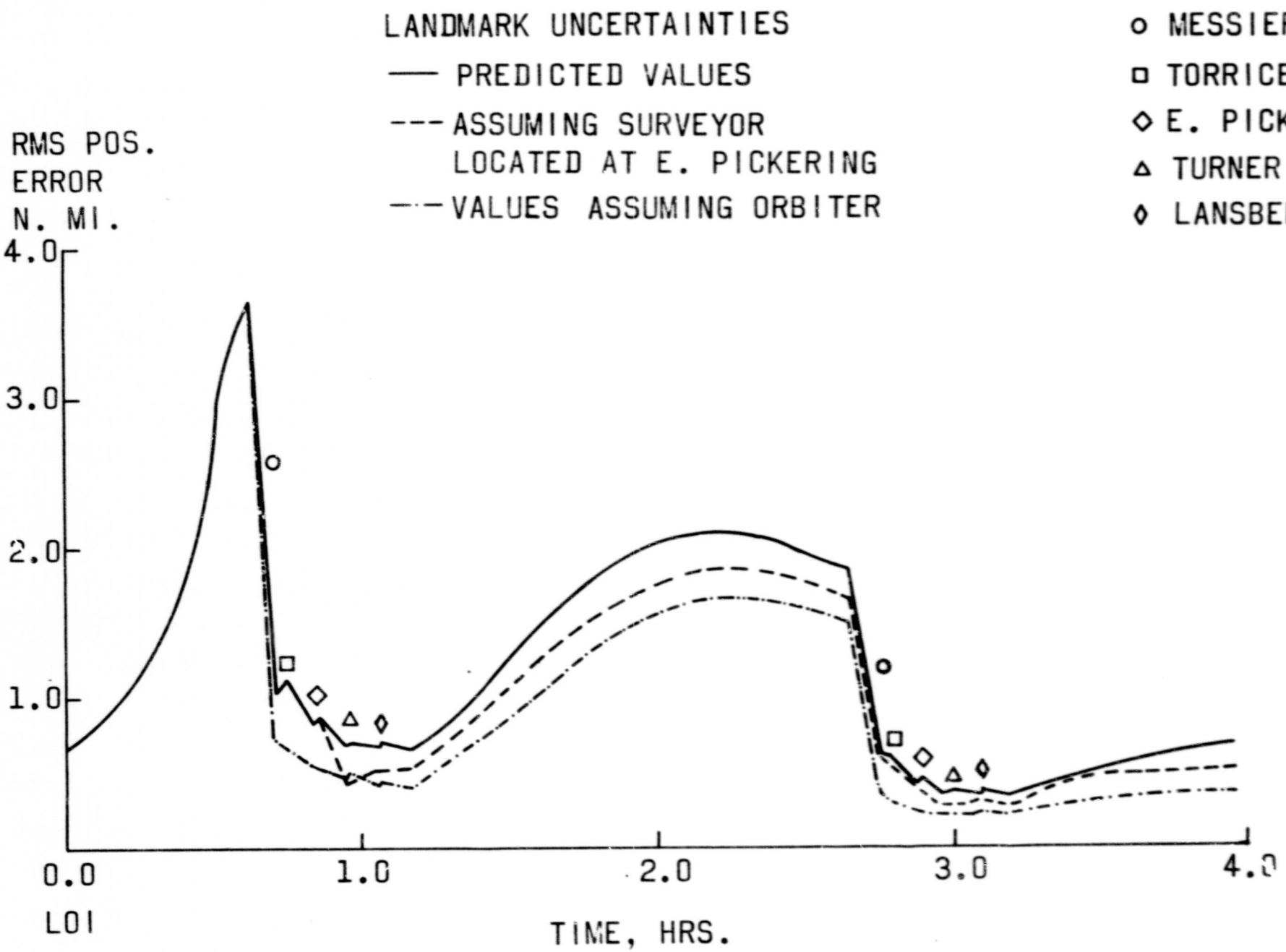

ONBOARD LUNAR ORBIT NAVIGATION CAPABILITY

FIGURE 4

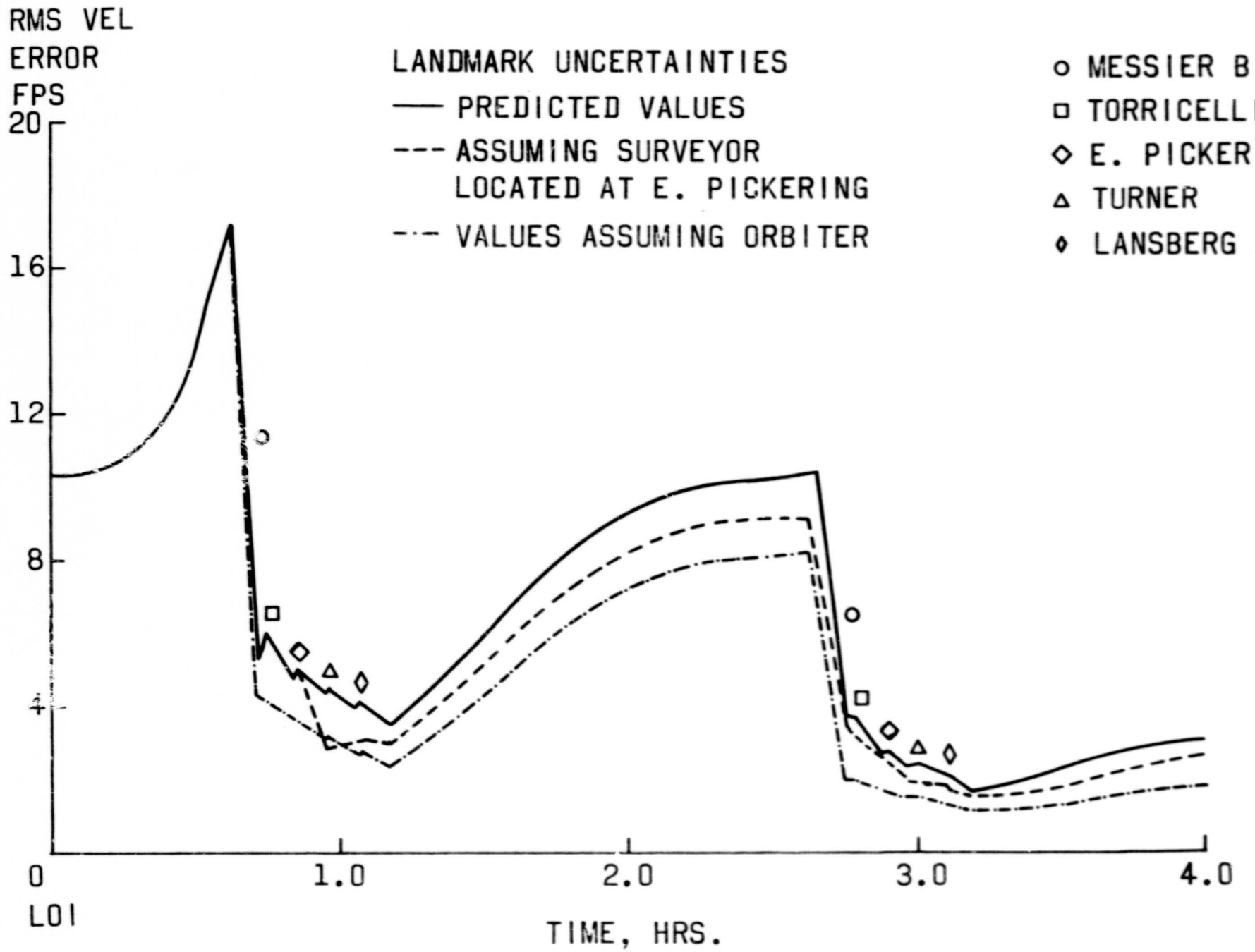

LANDING ACCURACY RESULTING FROM LUNAR ORBIT NAVIGATION

(TWO ORBITS, SCANNING TELESCOPE)

FIGURE 5

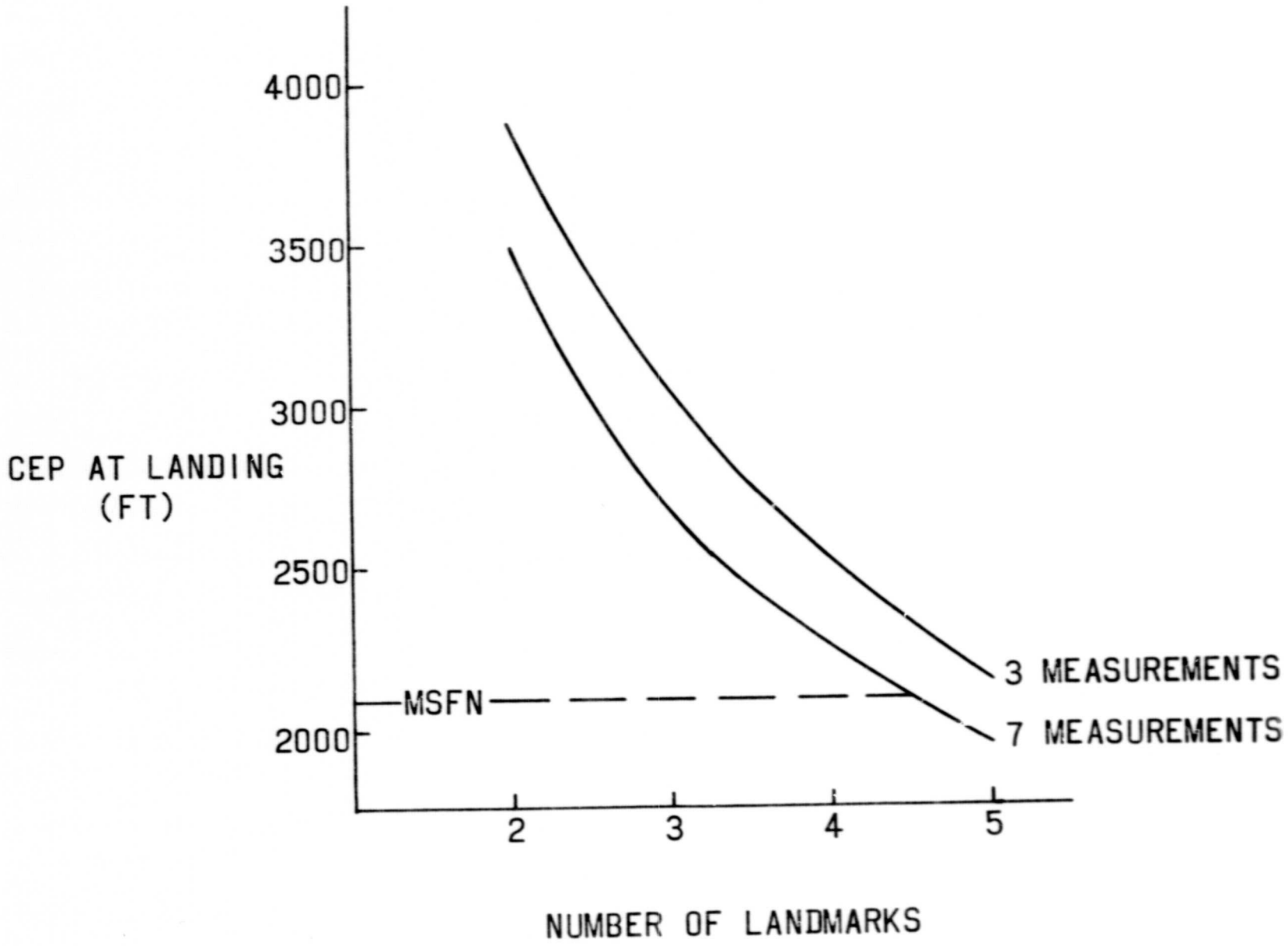

LUNAR ORBIT NAVIGATION CAPABILITY

FIGURE 6

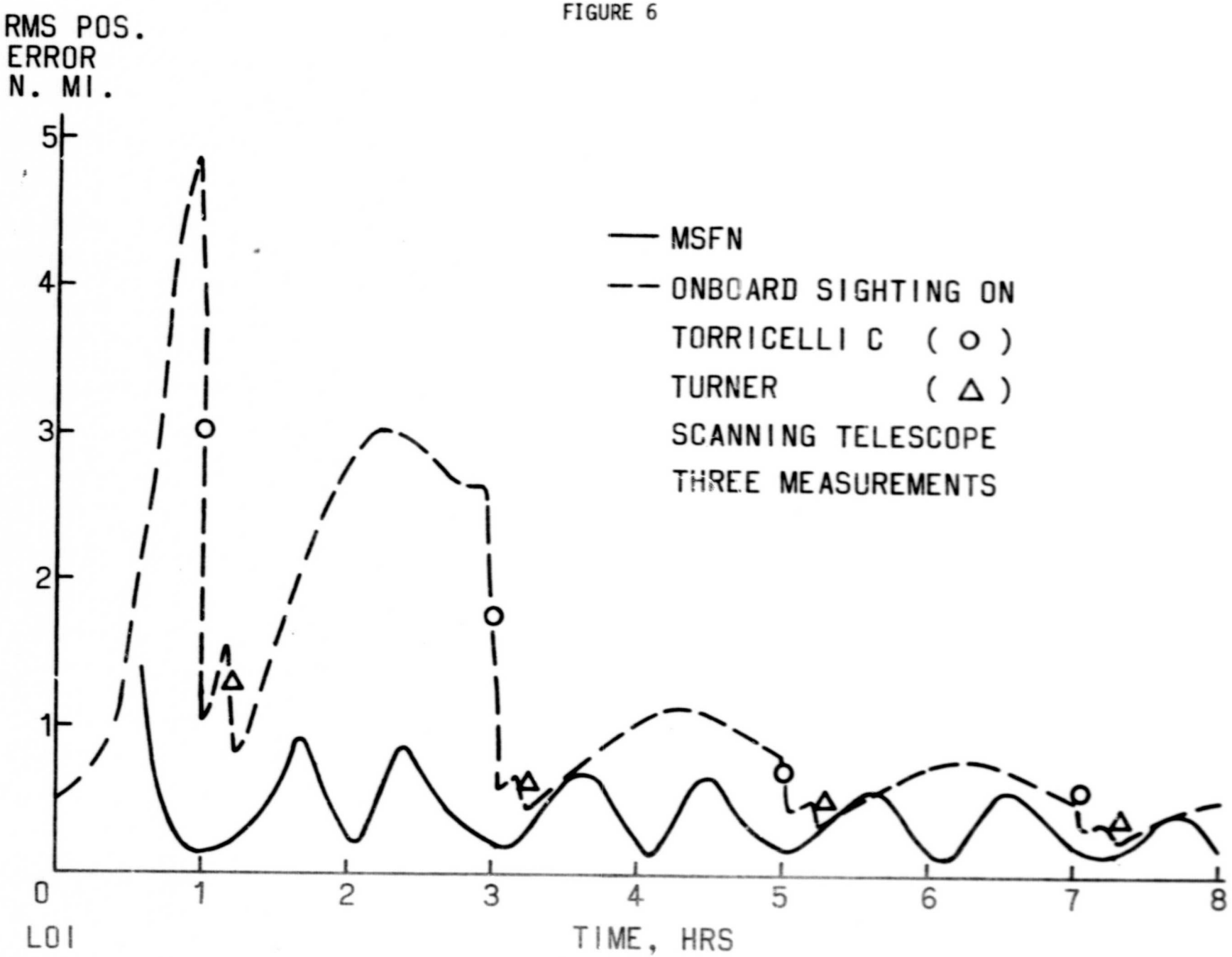

LANDING ACCURACY RESULTING FROM LUNAR ORBIT NAVIGATION (FT)
(FOUR ORBITS, THREE MEASUREMENTS, SCANNING TELESCOPE)

FIGURE 7

L.O.N.	σ RANGE	σ LATERAL	σ ALTITUDE	CEP (σ_R,σ_L)
ONBOARD TWO LANDMARKS	1776.	321.	694.	1240.
ONBOARD THREE LANDMARKS	1205.	285.	503.	868.
MSFN	2493.	549.	804.	1779.

LANDING ACCURACY RESULTING FROM
LUNAR ORBIT NAVIGATION (THREE ORBITS, THREE MEASUREMENTS)

FIGURE 8

UNITS-FEET		σ RANGE	σ LATERAL	σ ALTITUDE	CEP (σR, σL)
SCANNING TELESCOPE	TWO LANDMARKS	2835	539.4	1183	1988
	THREE LANDMARKS	2046	455.8	891.3	1412
SEXTANT	TWO LANDMARKS	1212	336.2	639.6	897.9
	THREE LANDMARKS	971.8	221.8	506.5	696.7
MSFN		2322	705.1	836.9	1752

GEOMETRY OF LANDING SITE DETERMINATION (LSD) BY ONBOARD SIGHTINGS

FIGURE 9

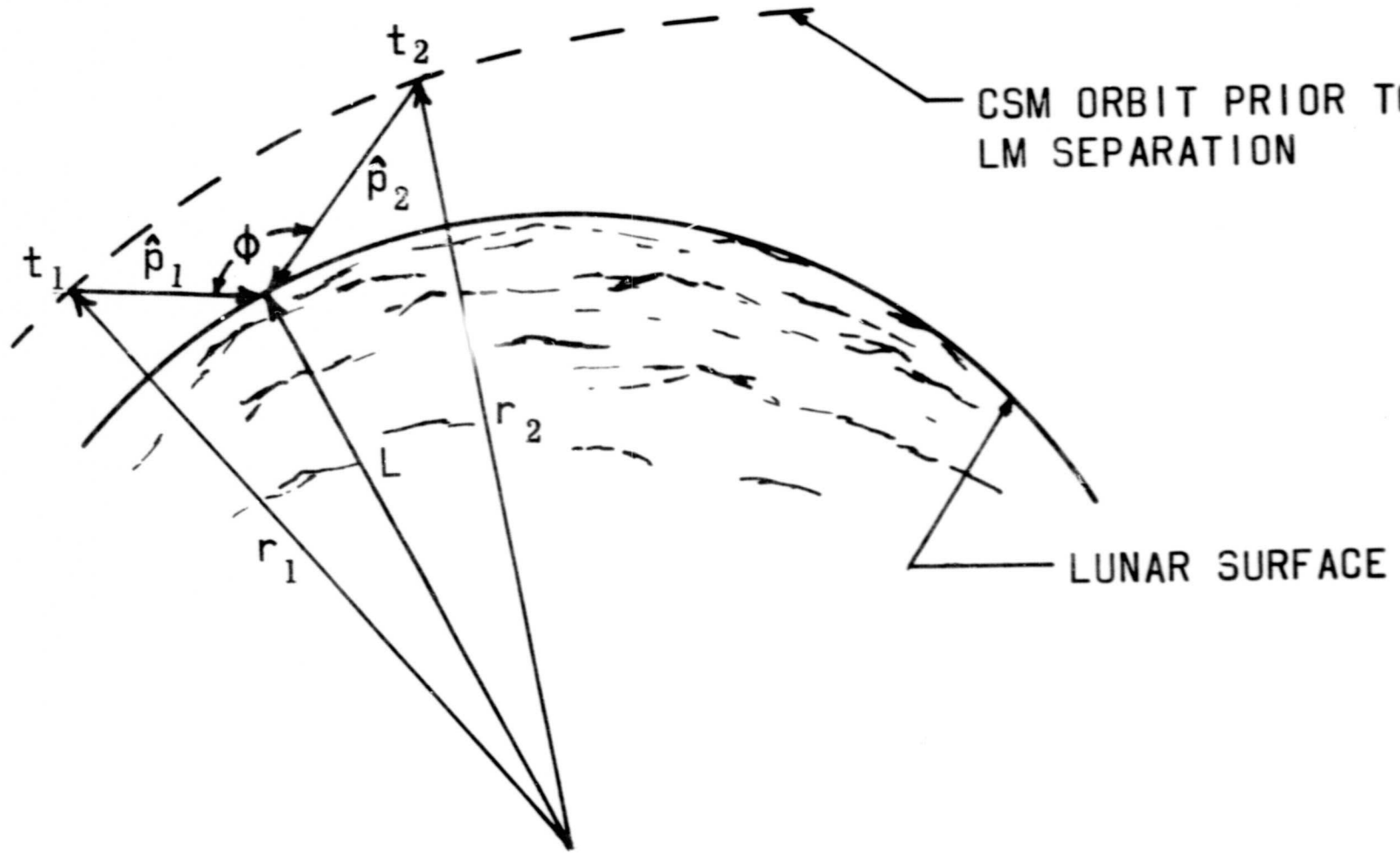

LANDING SITE UNCERTAINTIES

FIGURE 10

- PREDICTED BY TIME OF MANNED LUNAR LANDING (FOR 0, 0 LANDING SITE)

HOR = 1750 FT

VERT = 3215 FT

LUNAR RADIUS = 3281 FT

LIBRATION = 1641 FT

} ALT = 4877 FT

- LANDING SITE DETERMINATION WITH CSM ERRORS AS DETERMINED BY ONBOARD NAVIGATION (THREE ORBITS, TWO LANDMARKS)

LAT = 790 FT
LONG = 3490 FT
ALT = 1400 FT

- LANDING SITE DETERMINATION WITH CSM ERRORS AS DETERMINED BY MSFN NAVIGATION (3 ORBITS)

LAT = 1240 FT
LONG = 700 FT
ALT = 450 FT

LANDING ACCURACY RESULTING FROM
HOHMANN TRANSFER AND POWERED DESCENT (FT)

FIGURE 11

		σ RANGE	σ LATERAL	σ ALTITUDE	CEP (σR, σL)
AOT ALINEMENT ACCELEROMETER BIAS CALIBRATION	HOHMANN (45 SEC)	1068	61	540.9	727.8
	POWERED DESCENT	264.9	1412	1486	988.7
	TOTAL	1099	1413	1582	1478
LORS ALINEMENT BIAS CALIBRATION	HOHMANN	1003	39.5	539.7	682.6
	POWERED DESCENT	248.2	415.5	409	390.1
	TOTAL	1033	417.4	699.6	839
AOT ALINEMENT NO CALIBRATION	HOHMANN	3983	160.8	2142	2712
	POWERED DESCENT	782.8	1564	1679	1363
	TOTAL	4059	1572	2722	3257

TOTAL LANDING ACCURACY FOR THREE ORBITS (FT)

(TWO LANDMARKS, THREE MEASUREMENTS, SCANNING TELESCOPE, AOT, ACC. CAL.)

FIGURE 12

LANDING SITE ACCURACY		σ RANGE	σ LATERAL	σ ALTITUDE	CEP (σ_R,σ_L)
PREDICTED	ONBOARD	3506	2329	5261	3418
	MSFN	3106	2378	5195	3230
LSD	ONBOARD	4630	1710	2420	3700
	MSFN	2660	2000	1850	2730
PERFECT	ONBOARD	3040	1512	1975	2642
	MSFN	2569	1579	1789	2420

TOTAL LANDING ACCURACY (FT)

FIGURE 13

		σ RANGE	σ LATERAL	σ ALTITUDE	CEP (σR σL)
NO LANDING SITE DETERMINATION	LANDING SITE	1747	1747	4877	2951
	HOHMANN & POWERED DESCENT	1099	1443.1	1582	1478
	ON BOARD ORBIT NAVIGATION (2 LANDMARKS, 3 ORBITS)	2835	539	1183	1988
	MSFN (3 ORBITS)	2322	705.1	836.9	1752
	TOTAL ONBOARD	3506	2329	5261	3418
	TOTAL MSFN	3106	2373	5195	3230
LANDING SITE DETERMINATION	LANDING SITE (ONBOARD)	3490	790	1400	2340
	LANDING SITE (MSFN)	700	1240	450	1160
	TOTAL ONBOARD	4630	1710	2420	3700
	TOTAL MSFN	2660	2000	1850	2730

COMPARISON OF LM SIGHTING TECHNIQUES

FIGURE 14

TECHNIQUE	RCS PROP PER ORBIT	LM OBSERVATION TIME	COMMUNICATION LOSS
1. ROLL-YAW LV RATE	4.84 LB	4 MIN (3.4 MIN)(a)	2.3 MIN
2. ROLL LV RATE	4.61	4	9
3. PITCH LV RATE	4.94	3.4	4
4. ROLL INERTIAL (b) (c)	6.06	3.3	9
5. PITCH INERTIAL (b)	17.96	2.4	4
6. ROLL LM RATE (d)	7.81	15.3 (e)	INTERMITTANT
7. PITCH LM RATE	23.66	15.3	INTERMITTANT

NOTE: (a) LM IN SHAFT-TRUNION PLANE WOULD YIELD 3.4 MIN

(b) SHAFT AXIS ORIENTED TOWARD EACH LANDMARK

(c) 2 LM + LS, 6 LM + LS = 10.96 LB

(d) 2 LM + LS, AVE LM RATE = .25^{O}/sec

(e) IDEAL TIME FROM HORIZON TO HORIZON

OPTICS LOOK ANGLE (LOCAL VERTICAL RATE)

FIGURE 15

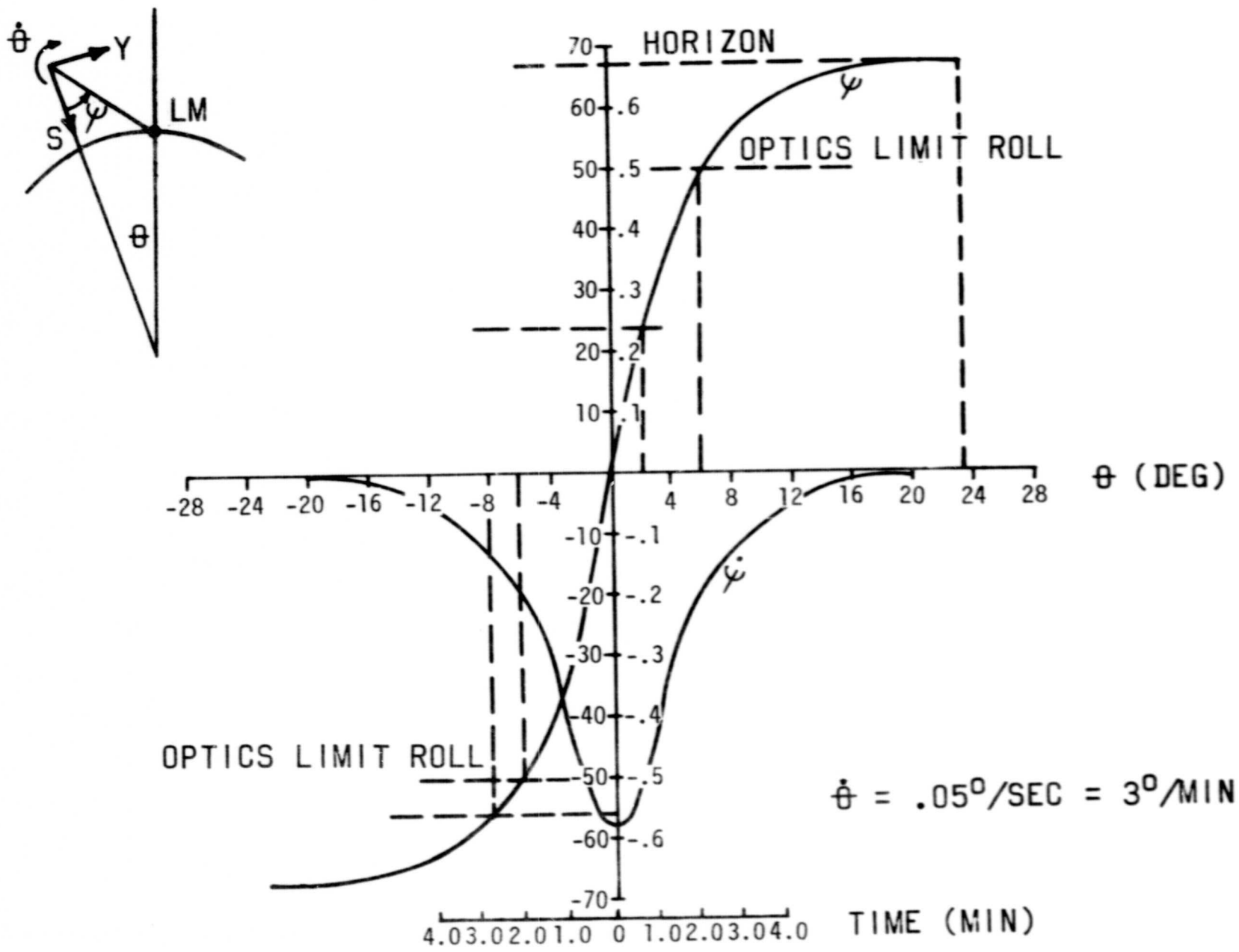

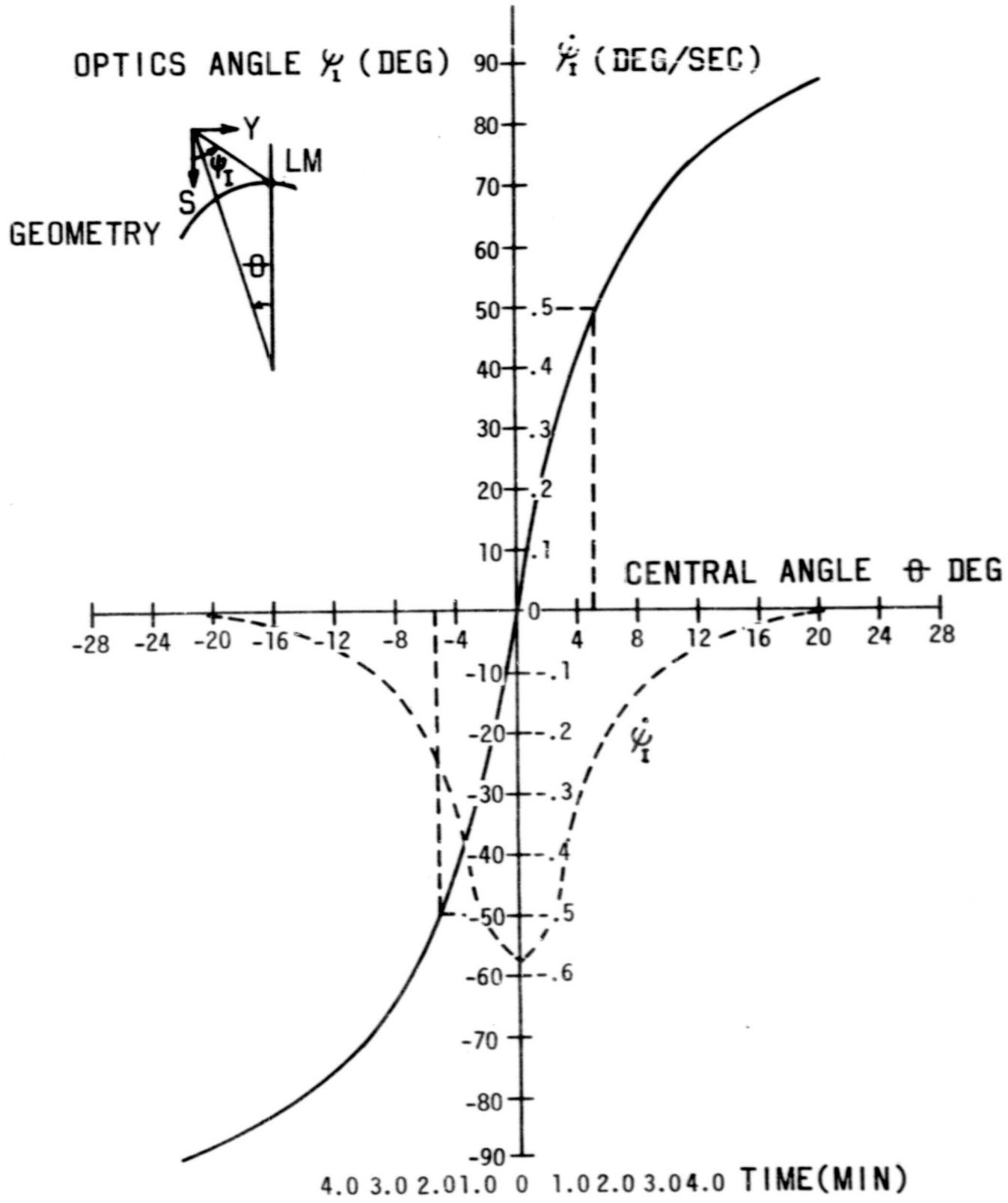

OPTICS LOOK ANGLE
(INERTIAL)

FIGURE 16

RCS PROPELLANT REQUIREMENTS

FIGURE 17

ROLL-YAW AT LOCAL VERTICAL RATE(.05°/SEC)

PROP PER ORBIT

	FUNCTION	LONG	SYS	MANEUVER	RATE	TIME	PROP
1.	IMU ALINE	+90°	(SCS MANUAL)	PITCH-ROLL	.5°/SEC	6MIN	4.46 LB
2.	START LV RATE	+89°	G&N AUTO	ROLL	.04		.02
				YAW	.03		.12
3.	STOP LV RATE	-7.5°	G&N AUTO	ROLL	.04		.02
				YAW	.03		.12
	ATTITUDE HOLD (.5°DB) +90°L TO -7.5° LONG (.54 HR) (.54)·(.19)=						.10
	PROP PER ORBIT FOR NAV SIGHTING=						4.84 LB
4.	COMM. (REQD. IN NOMINAL PROFILE)	-7.5°	SCS	PITCH-ROLL	.5°/SEC		4.46 LB

IMPACT ON RCS PROPELLANT BUDGET

FIGURE 18

	NAA BASELINE BUDGET	MSC CRITERIA	TRW AUSTERE
NOM	453	774	206
SIGHT IN BUDGET	-22	-119	-0
SIGHT ON 2 ORBITS	+10	+10	+10
(ROLL-YAW LV)	441	665	216
NOM	-2%	-13%	+5%

ATTITUDE
TIMELINE

FIGURE 19

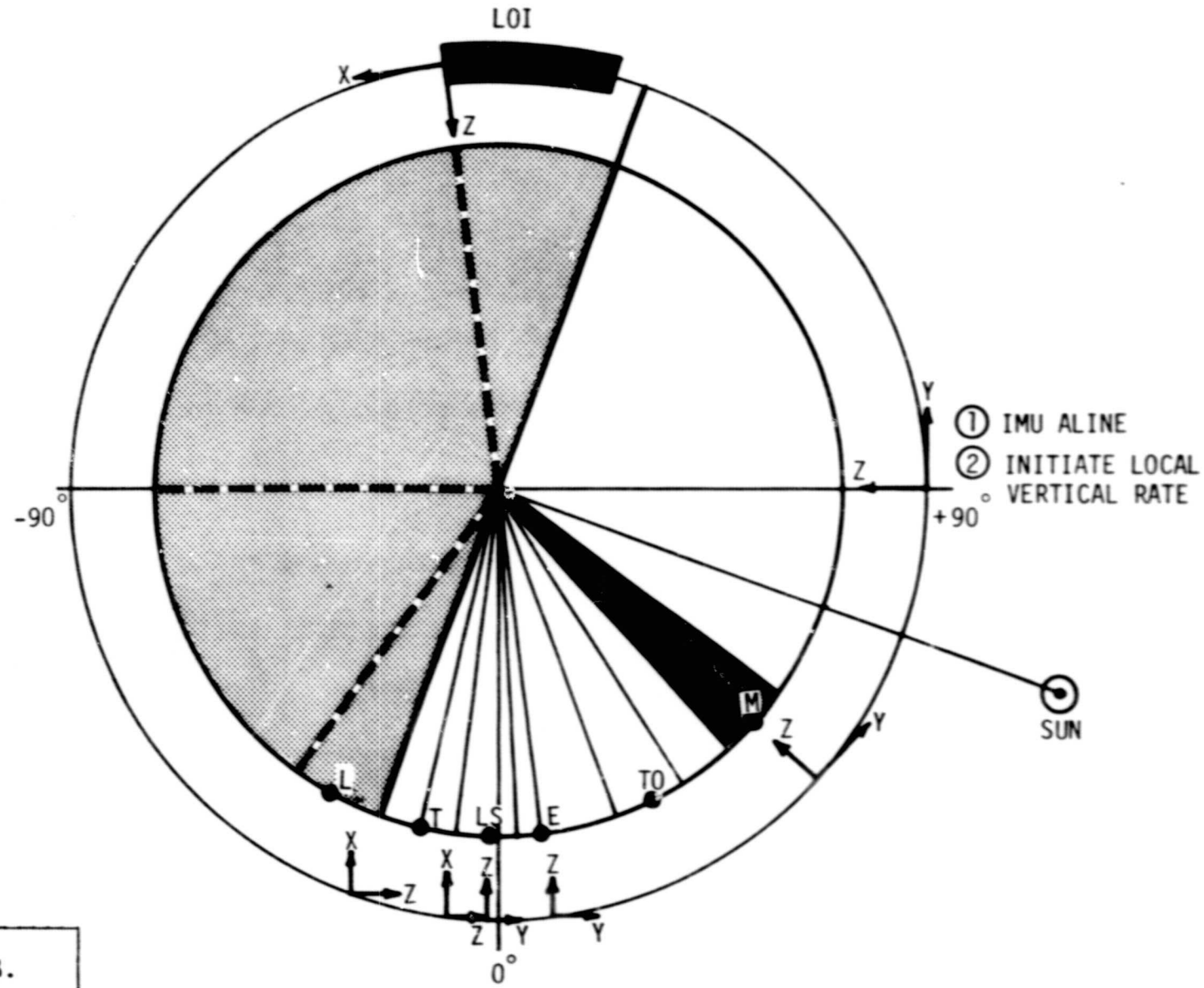

M	MESSIER B.
TO	TORRICELI C.
E	PICKERING E.
LS	LANDING SITE
T	TURNER
L	LANSBERG D.

③ STOP LV RATE

④ SCS YAW-ROLL FOR LUNAR OBSERVATION & COMMUNICATION

AQUIRE COMM

LOSE COMM
-33° PITCH

2.3 MINUTES

LANDMARK SIGHTING GEOMETRY

FIGURE A1

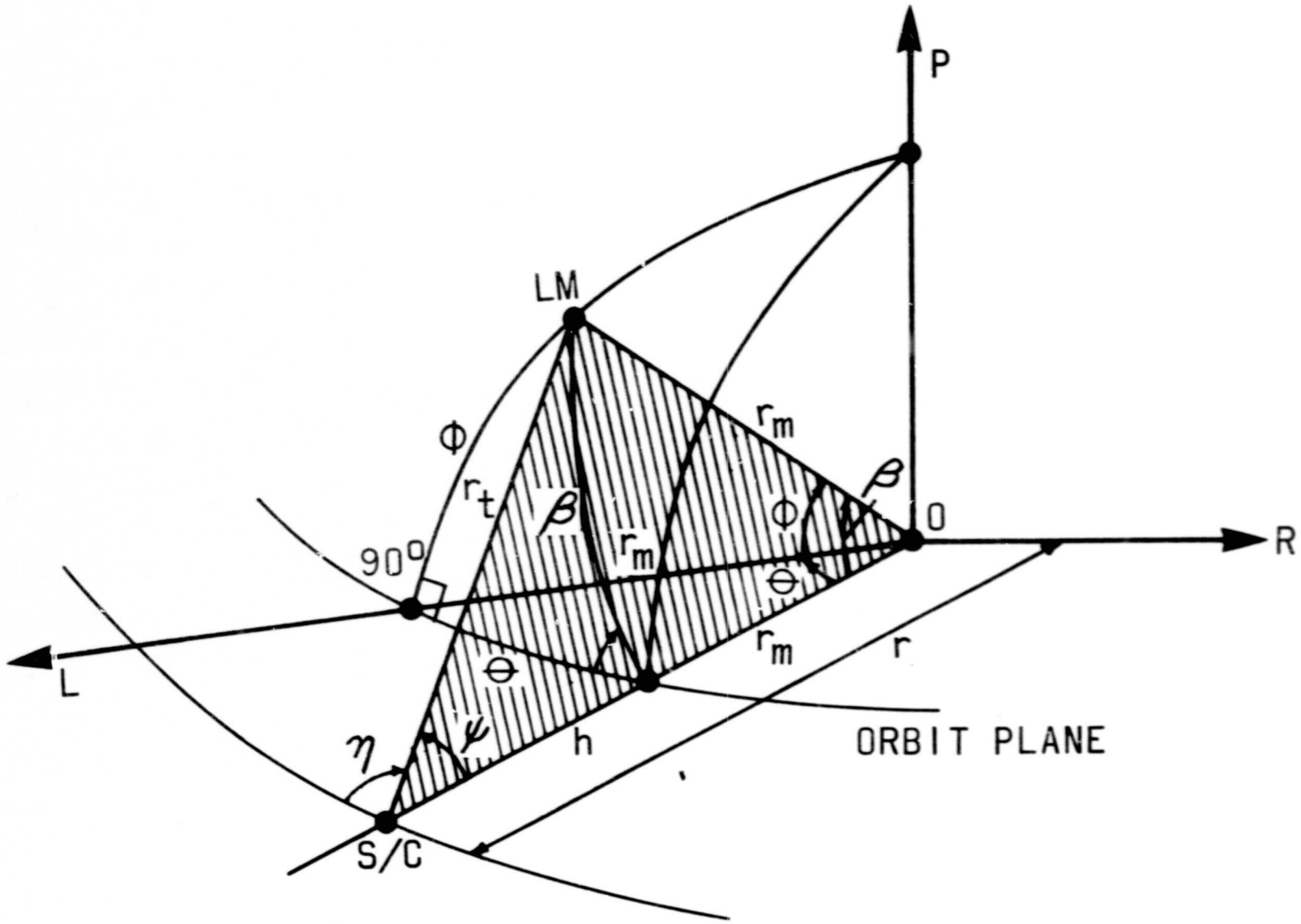

OPTICS LOOK ANGLE
(INCLUDING OUT OF PLANE ANGLE ϕ)

FIGURE A2